PHYS 7363 - Experimental Particle Detection and Detectors I

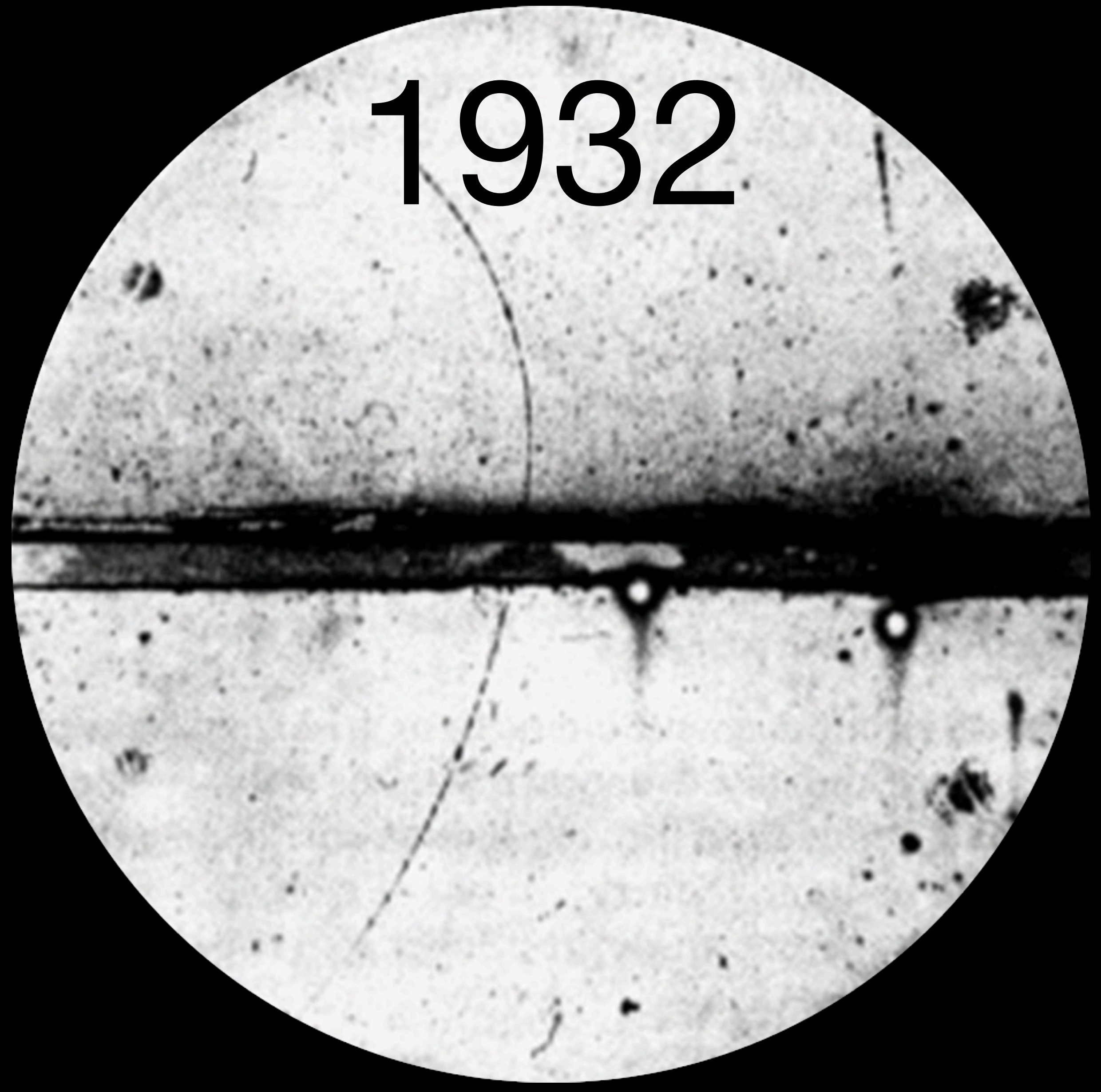

Particle detectors are the workhorses of experimental physics. In this course, we'll dive deep into their physics, exploring the incredible evolution of our experimental techniques over the past nine decades. You'll gain a solid understanding of *particle detection* and *identification*, examine the intricate designs of modern detectors, and learn how machine learning is being harnessed to push the boundaries of detector design. If you're intrigued by how we “see” subatomic particles, this course is for you!

2017

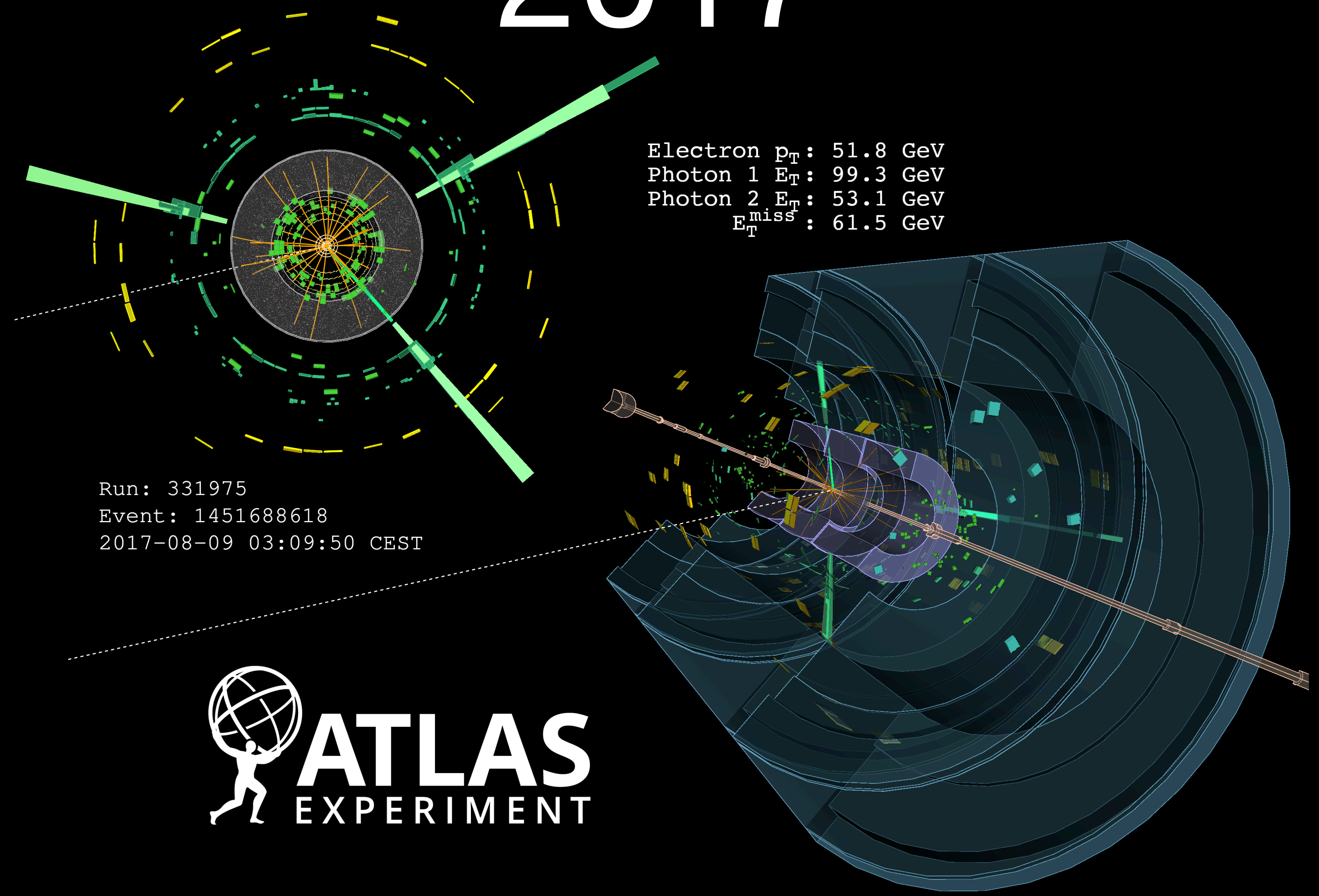

Detect Identify Measure

To discuss prerequisites (and any questions on the content of the course), please contact me: saptaparnab@smu.edu

Schedule

Month	Monday	Tuesday	Wednesday	Thursday	Friday	Saturday	Sunday
August	18	19	20	21	22	23	24
	25 ✅	26	27	28	29 ✅	30	31
September	1	2	3 ✅	4	5 ✅	6	7
	8 ✅ 1.5 hours	9	10	11	12	13	14
	15 ✅ 1.5 hours	16	17 ✅ 1.5 hours	18	19 ✅ 1.5 hours	20	21
	22 ✅ 1.5 hours	23	24 ✅ 1.5 hours	25	26 ✅ 1.5 hours	27	28
October	29 ✅ 1.5 hours	30	1 ✅ 1.5 hours	2	3 ✅ 1.5 hours	4	5

Schedule

Month	Monday	Tuesday	Wednesday	Thursday	Friday	Saturday	Sunday
October	6 ✅ 1.5 hours	7	8	9	10	11	12
	13	14	15	16	17	18	19
	20	21	22	23	24	25	26
	27	28	29	30	31	1	2
November	3	4	5	6	7	8	9
	10	11	12	13	14	15	16
	17	18	19	20	21	22	23
	24	25	26	27	28	29	30
December	1	2	3	4	5	6	7
	8	9	10	11	12	13	14

Schedule

- Midterm on October 27th
- We decided on continue with this 80 min long lectures thrice a week
  - We will continue with this schedule unless I think that we don’t need to meet for that long a time frame
  - Next week, I am away at a conference, so we will meet on Monday as planned in person, Wednesday would be a zoom lecture and no lecture on Friday

$$\eta = -\ln\left[\tan\left(\frac{\theta}{2}\right)\right]$$

ATLAS and CMS Calorimeters

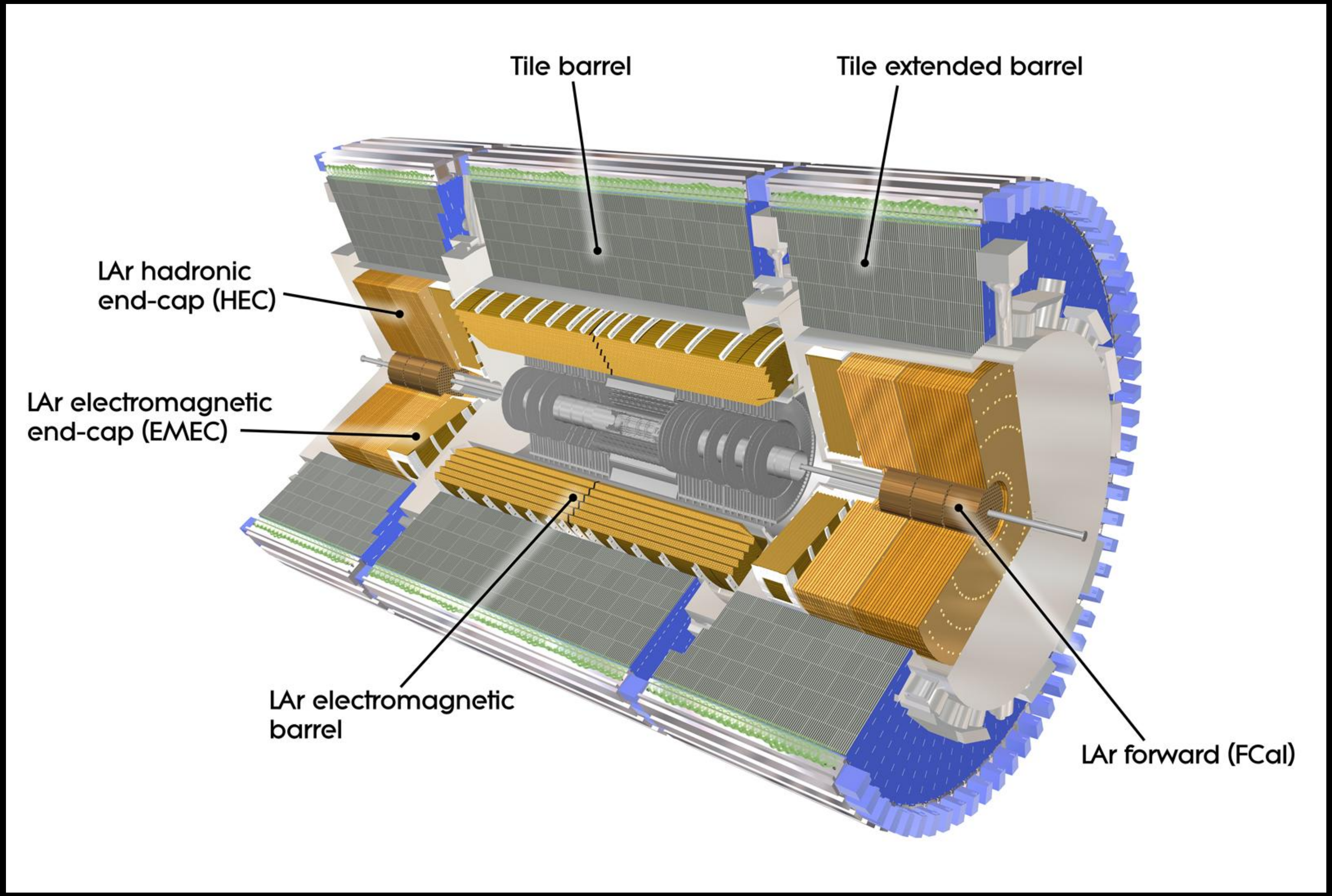

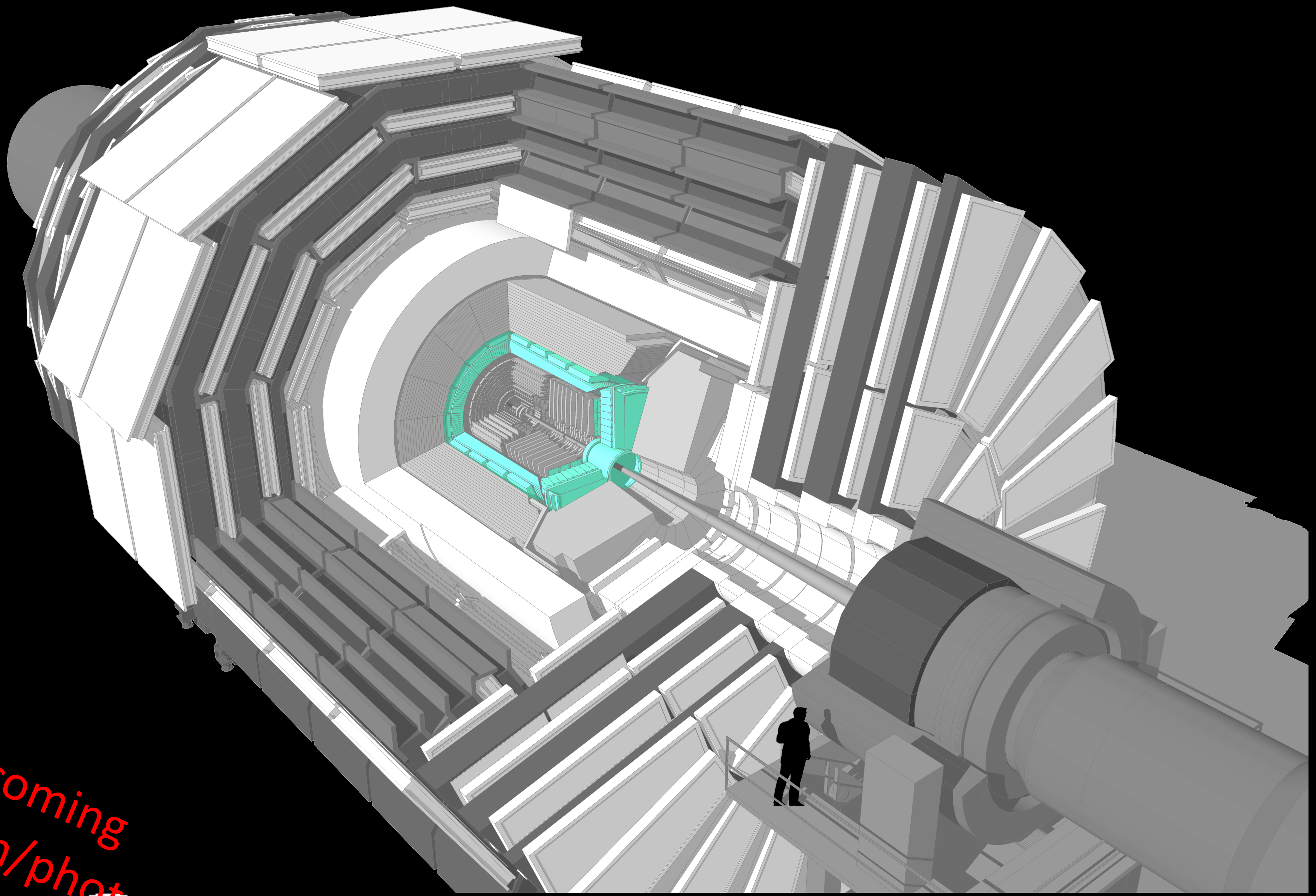

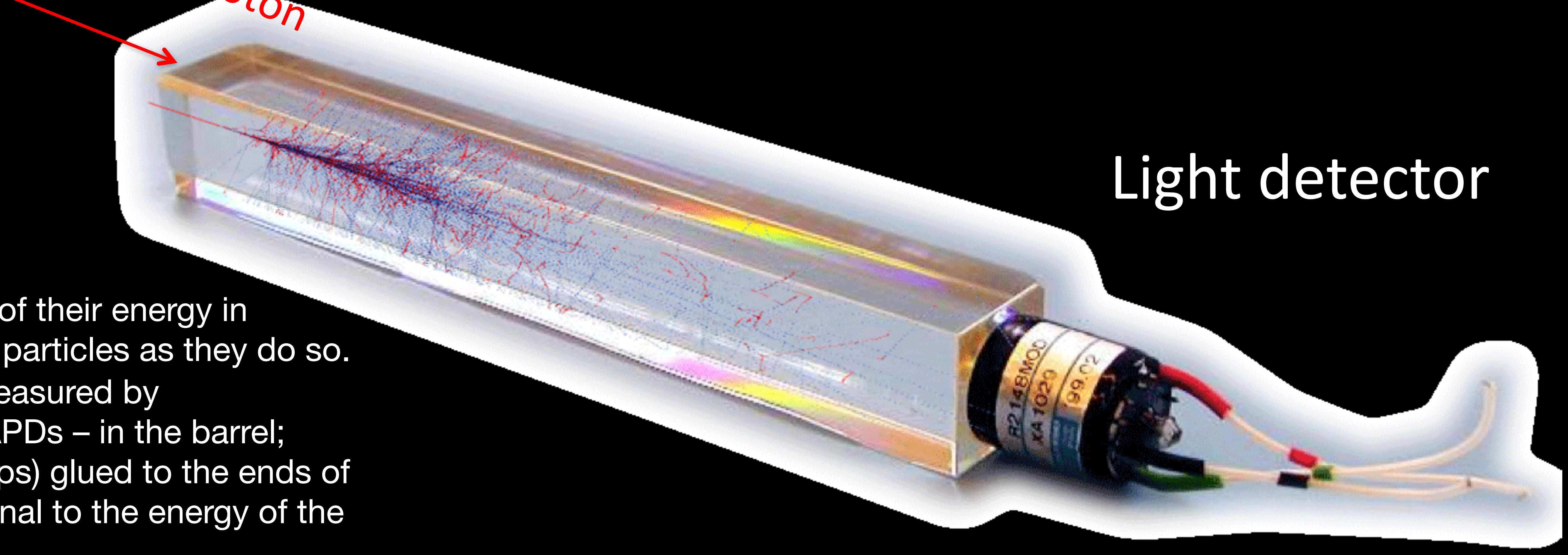

Incoming electrons and photons release all of their energy in the $PbWO_4$ crystals, producing a shower of particles as they do so. Light is also produced in the shower and measured by photodetectors (avalanche photodiodes – APDs – in the barrel; vacuum phototriodes – VPTs – in the endcaps) glued to the ends of the crystals; the amount of light is proportional to the energy of the electron/photon: more energy = more light.

Homogeneous calorimeter

Convert energy E of incident particles to detector response

$$S \propto E$$

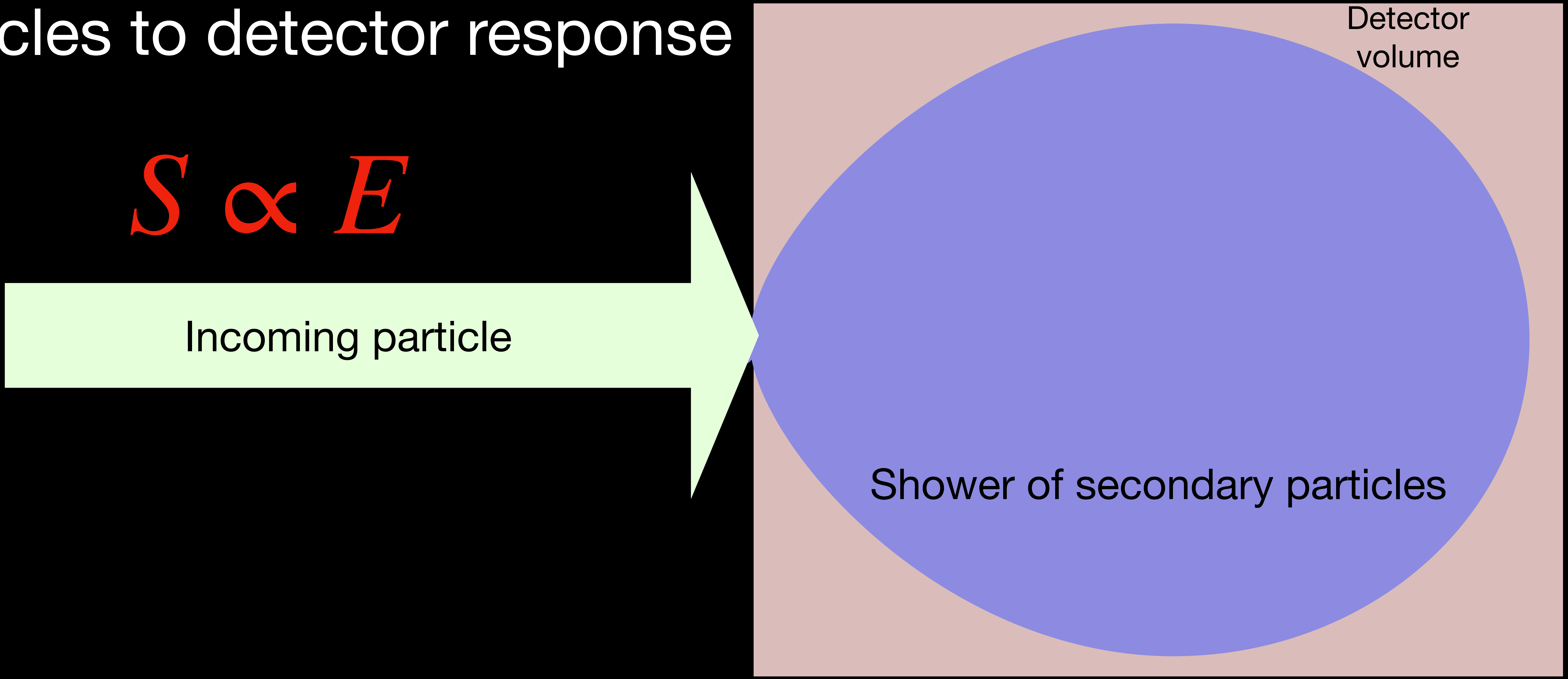

This is a homogenous calorimeter — think of lead tungstate ECAL in CMS

Sampling calorimeter

Convert energy E of incident particles to detector response

$$S \propto E$$

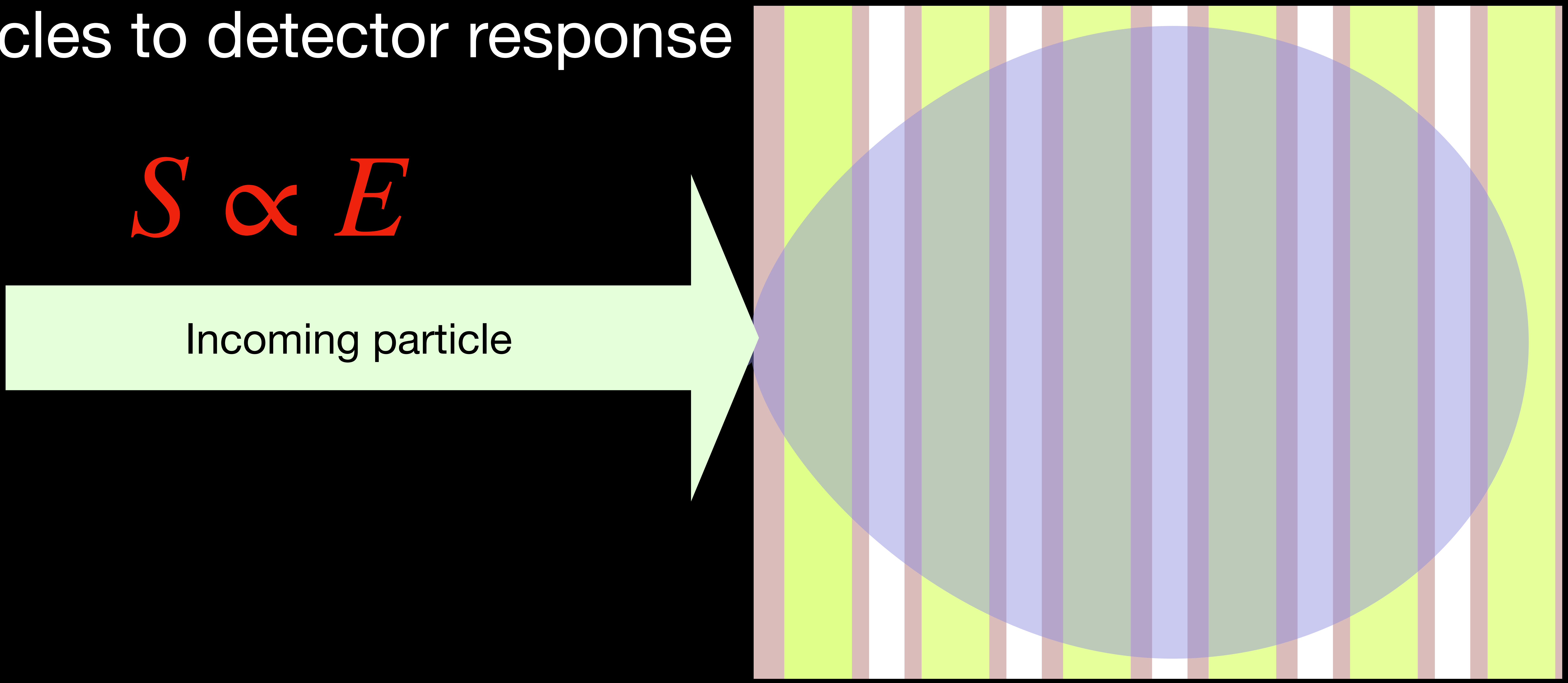

Incoming particle

Detector volume

Interleaved with passive absorber material and active detectors

Shower of secondary particles

This is a sampling calorimeter — think of HighGranularity Calorimeter in CMS

Calorimeter

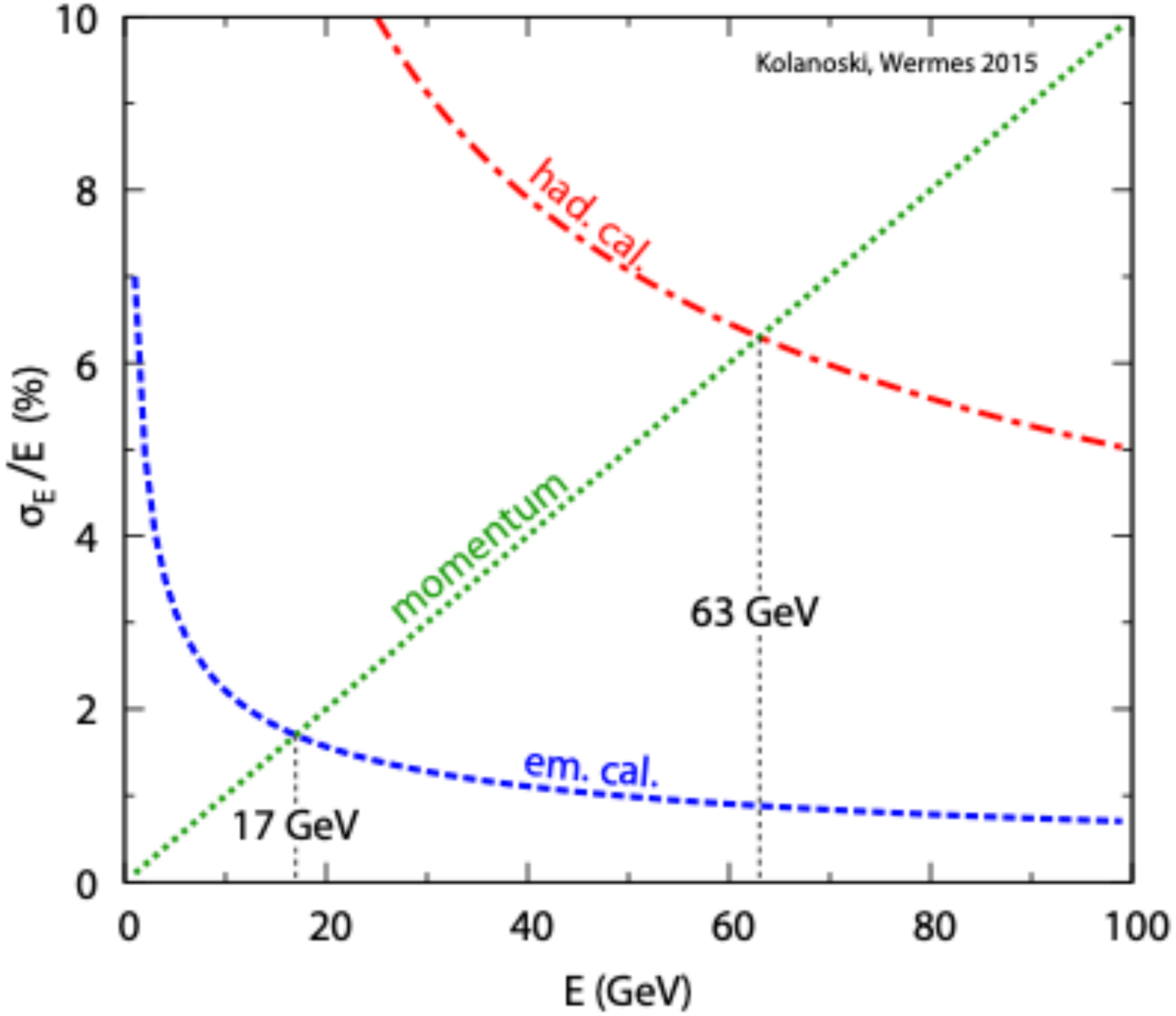

Fig. 15.1 Comparison of typical energy resolutions in a detector. In the example the energy resolutions of electromagnetic and of hadronic calorimeters are assumed to be $\sigma_E^{em}/E = 7\,\%/\sqrt{E}$ and $\sigma_E^{had}/E = 50\,\%/\sqrt{E}$, respectively. For the energy determination by momentum measurement a momentum resolution of $\sigma_p/p = 0.1\,\%\,p$ is assumed. With these values the energy determination by calorimetric measurements becomes better than by momentum measurements at 17 GeV and 63 GeV, respectively.

Energy resolution — Photons

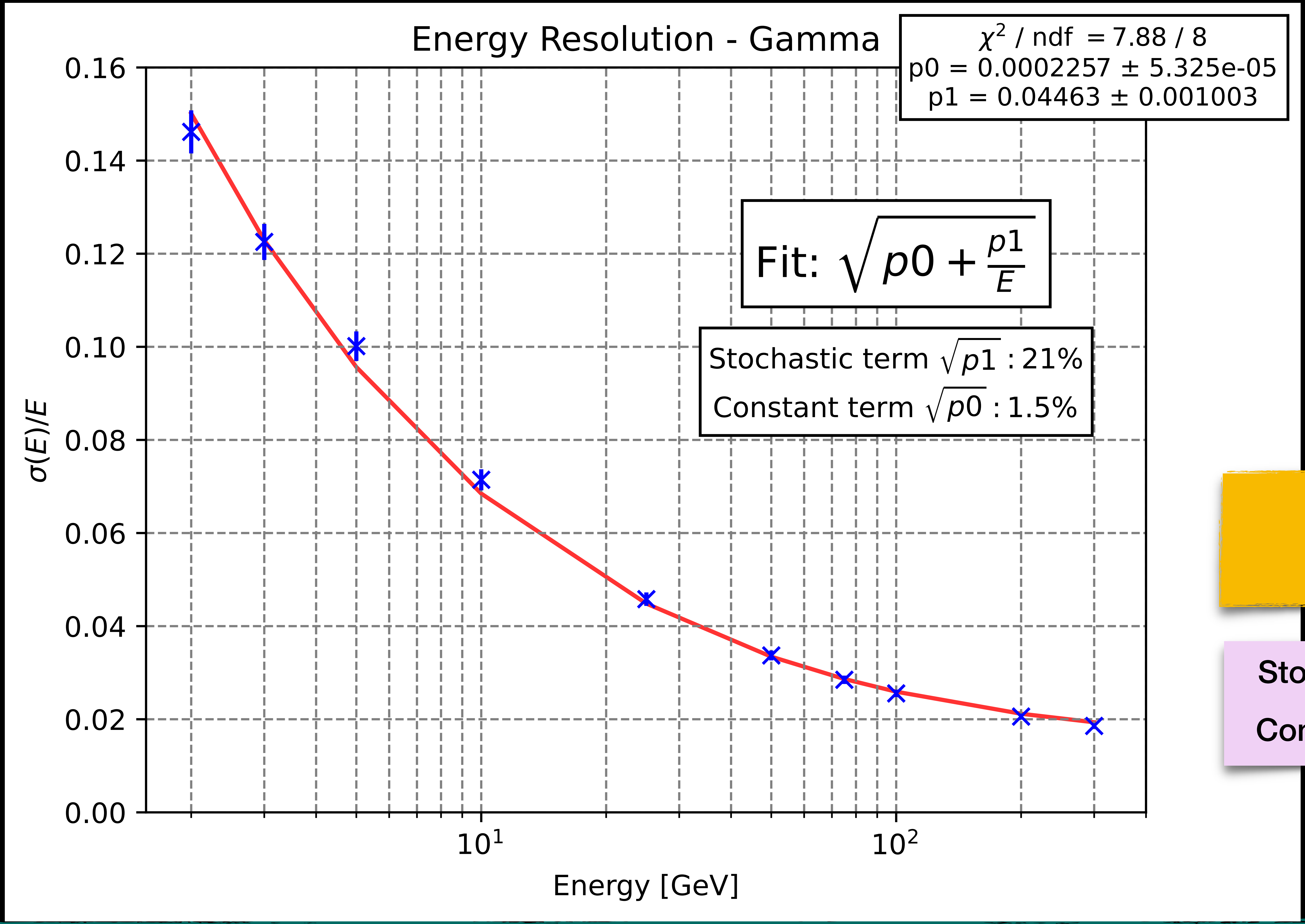

Excellent efficiency of reconstructing low energy clusters

Fit: $\sqrt{p_0 + \frac{p_1}{E}}$

Stochastic term $\sqrt{p_1}$: 21 %

Constant term $\sqrt{p_0}$: 1.5 %

Calorimeter

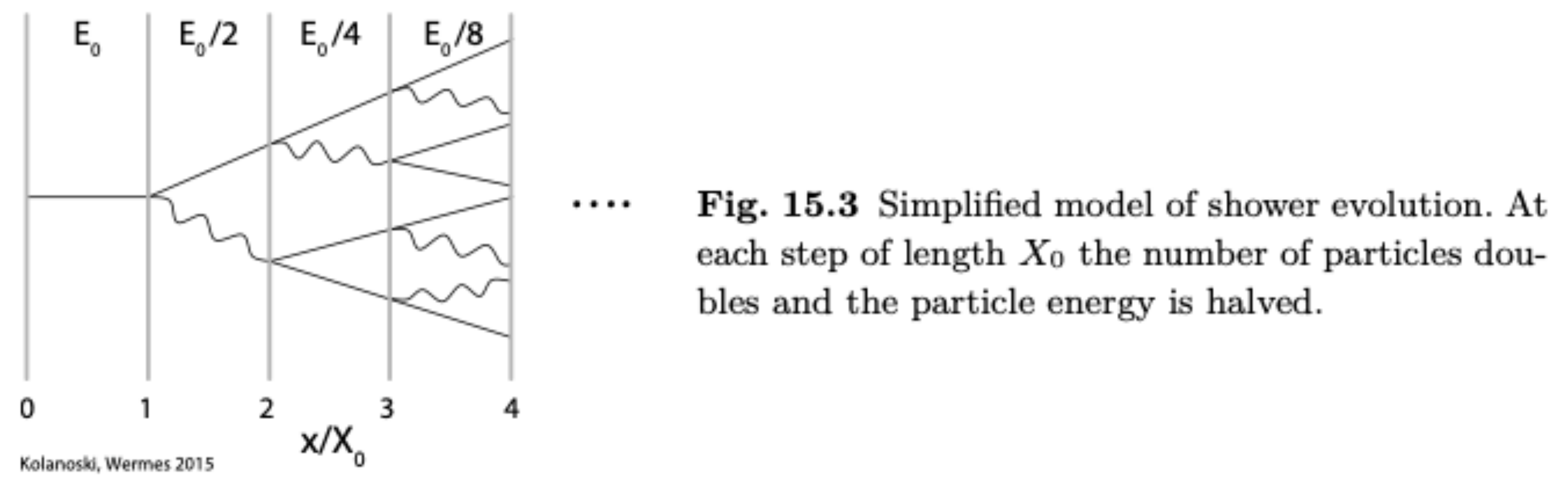

Kolanoski, Wermes 2015

Fig. 15.3 Simplified model of shower evolution. At each step of length X_0 the number of particles doubles and the particle energy is halved.

Calorimetry

- Distance $s = tX_0$ (t is the path length in units of radiation length)
- The maximum number and energy of particles are: $N = 2^t$, $E = \dfrac{E_0}{2^{t_{max}}}$
- $N_{max} = \dfrac{E_0}{E_c}$, $t_{max} = \dfrac{\ln E_0/E_c}{\ln 2}$

- Homogeneous Calorimeters: Lead Tungstate ($PbWO_4$) Crystals
- This technology, used by the CMS experiment, is designed for the best possible energy resolution. Principle: The entire detector volume is made of a single, dense, scintillating material. The lead tungstate crystal acts as both the material where the particle shower develops (the absorber) and the material that generates the signal (the active medium).
- High Density & Short Radiation Length: $PbWO_4$ is extremely dense (8.3 g/cm^3) with a very short radiation length (X_0 = 0.89 cm). This allows for a very compact calorimeter that can contain the entire electromagnetic shower of even very high-energy particles within a relatively short depth (~25 cm).
- Signal Generation: The signal is scintillation light. As shower particles traverse the crystal, they excite the atoms, which then de-excite by emitting photons.
- Low Light Yield but Fast Response: A key feature of $PbWO_4$ is its relatively low light yield compared to other crystals like CsI(Tl). However, its scintillation light is emitted very quickly (about 80% within 25 ns). This fast response is crucial for handling the high event rates at the LHC. The low light yield means a photodetector with internal gain, like an Avalanche Photodiode (APD) or Vacuum Phototriode (VPT), is required for readout.
- Excellent Energy Resolution: Because the entire shower energy is converted into a detectable signal (with no sampling fluctuations), the primary limit on resolution comes from the statistics of the scintillation photons. This leads to outstanding energy resolution, especially at high energies where the constant term from calibration and non-uniformities is the limiting factor. The CMS ECAL achieves a resolution with a stochastic term of $a \approx 2.8\% \sqrt{GeV}$.
- Radiation Hardness: This specific crystal material was developed to be highly resistant to the extreme radiation environment at the LHC.

- Sampling Calorimeters: Lead & Liquid Argon (Pb/LAr)

- This technology, used by the ATLAS experiment, is designed for high granularity, stability, and robust operation.
  Principle: This is an inhomogeneous detector. It consists of alternating layers of a dense absorber material (lead plates) and a separate active medium (liquid argon). The shower develops primarily in the lead, and the charged particles are then "sampled" as they cross the liquid argon gaps.

- Signal Generation: The signal is ionization charge. As shower particles pass through the liquid argon, they ionize the argon atoms, creating electron-ion pairs. An applied high voltage drifts these electrons to segmented electrodes, inducing a current signal.

- Accordion Geometry: The ATLAS calorimeter uses a unique accordion-like shape for its lead plates and electrodes. This allows for a completely hermetic design (no cracks) in the azimuthal direction and enables fast signal readout since the connections are at the front and back, not on the sides.

- High Granularity: Because the signal is collected on finely segmented electrodes, it is relatively easy to achieve very high granularity both laterally and longitudinally (in depth). This is excellent for distinguishing electrons from jets, identifying photons from π^0 decays, and precisely measuring the shower position and direction.

- Intrinsic Radiation Hardness & Stability: Liquid argon is an intrinsically radiation-hard active medium. Its response does not degrade over time, and it is very stable in its properties, simplifying calibration.

- Good, but Not Superior, Energy Resolution: The energy resolution is fundamentally limited by sampling fluctuations. Since only a fraction of the total shower energy is deposited in the active medium, there are statistical fluctuations in how much energy is sampled in each event. This leads to a larger stochastic term in the resolution formula compared to a homogeneous crystal calorimeter. The ATLAS ECAL achieves a resolution with a stochastic term of a $\approx 10\% \sqrt{\text{GeV}}$.

Longitudinal shower profile

- The dimensions of showers determine the construction of calorimeters
- An empirical formula for the longitudinal energy distribution of a shower was derived by Longo and Sestili:
  - $\frac{dE}{dt} = E_0 \frac{b^a}{\Gamma(a)} t^{a-1} e^{-bt}$
  - Parameters a and b depend on the total energy deposited (E_0) and Z and Γ is the gamma function
  - Shower maximum $t_{max} = \frac{a-1}{b}$

Longitudinal shower profile

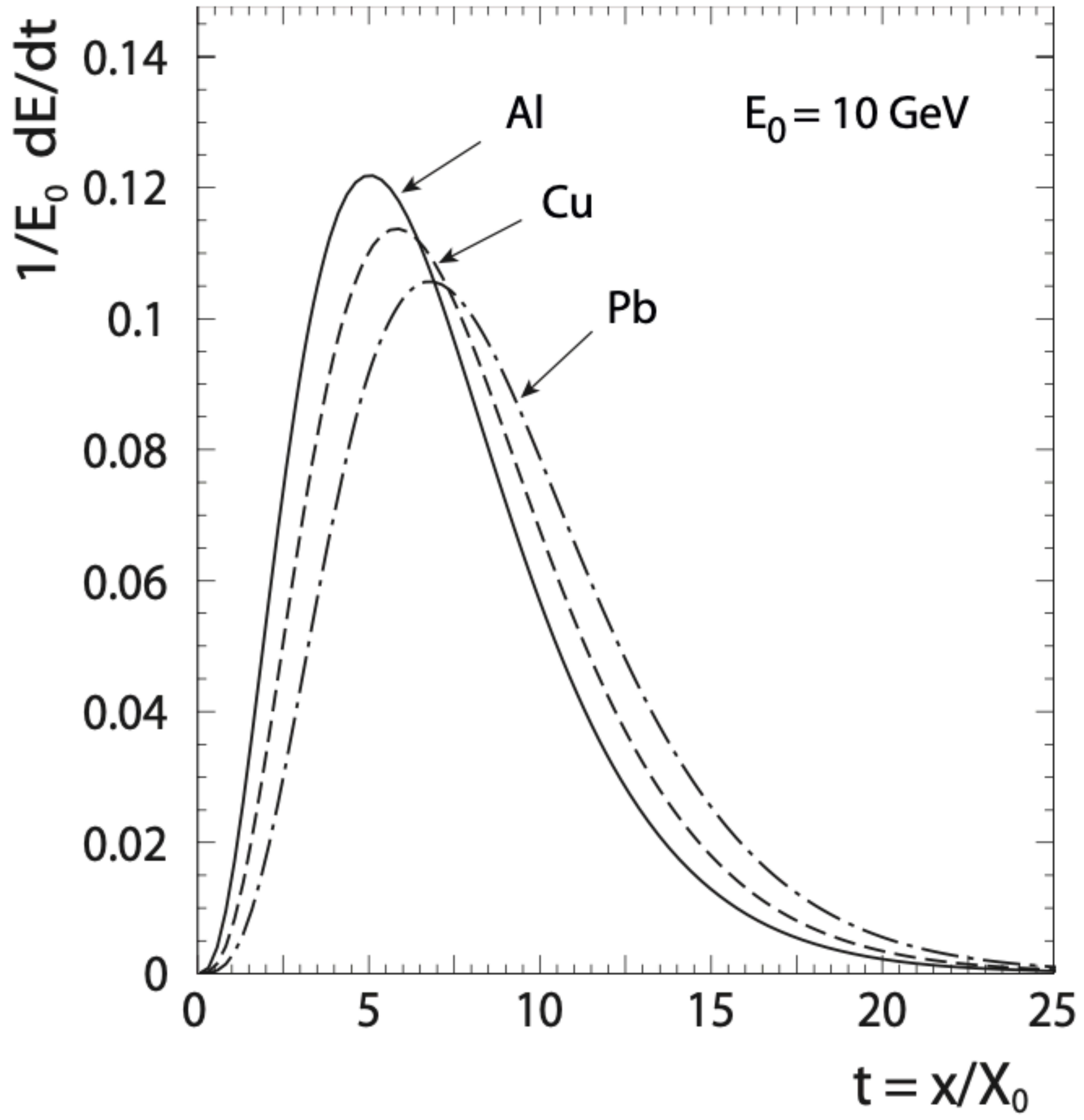

Fig. 15.4 Longitudinal profiles of 10-GeV electron showers calculated according to the Longo formula (15.17) for three different materials. The parameters are: $b = 0.5$, the same for all materials, and a calculated from (15.18) and (15.19). Due to the normalisation factor $1/E_0$ the area under each curve is the same. The differences in the shower development are due to the different critical energies of the three materials (see table 3.4).

Lateral shower profile

- At high energies, two shower processes scatter particles under a very small angle, naturally showers do not extend much laterally
- Lateral profile determined by other factors like multiple scattering of low energy charged particles
- Follow details of lateral shower profiles in Fig. 15.6 of the book and the accompanying section

Comparison of electromagnetic and hadronic showers

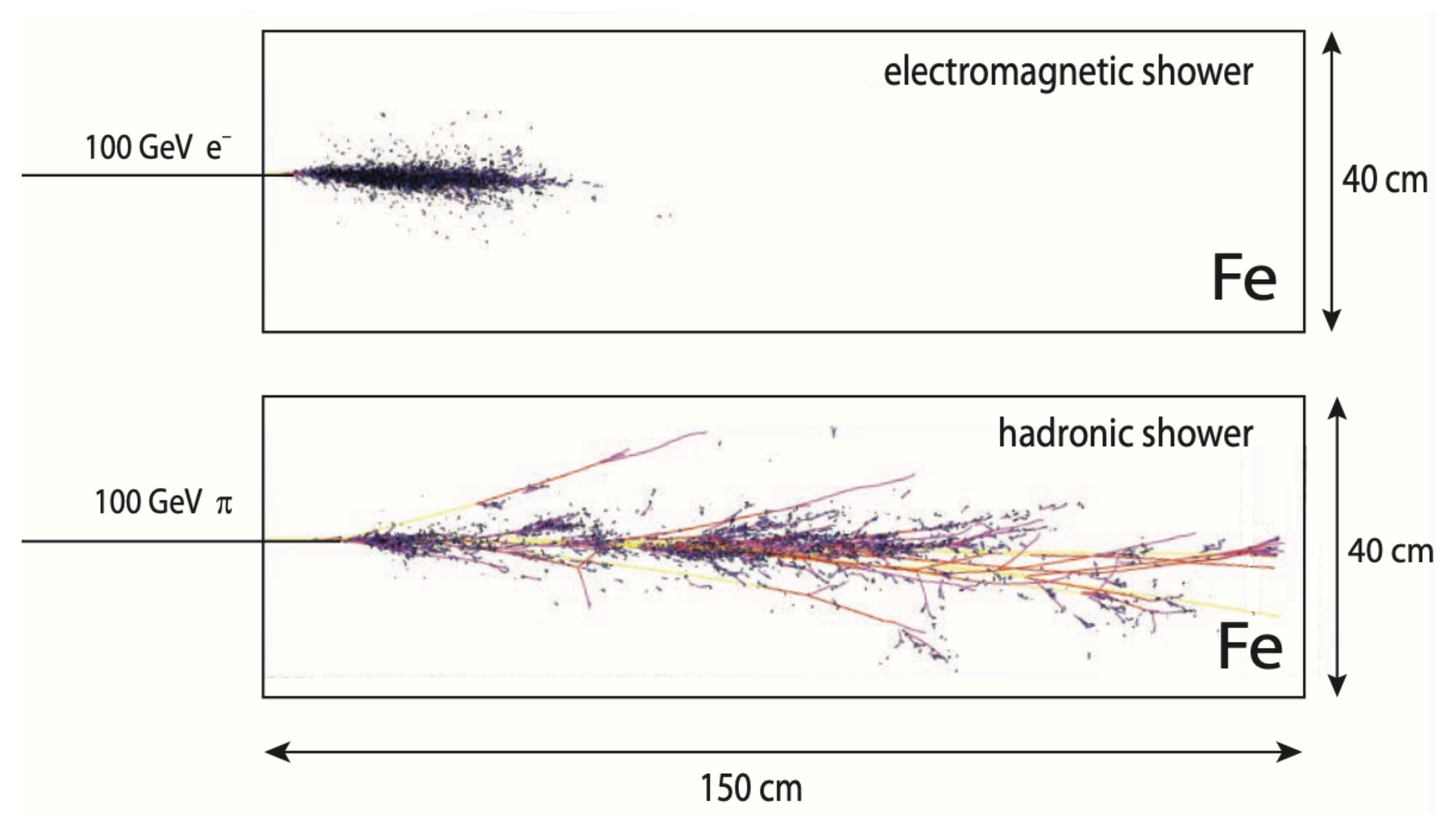

Shower visualization tool

- Visualize showers: https://www.iap.kit.edu/corsika/index.php

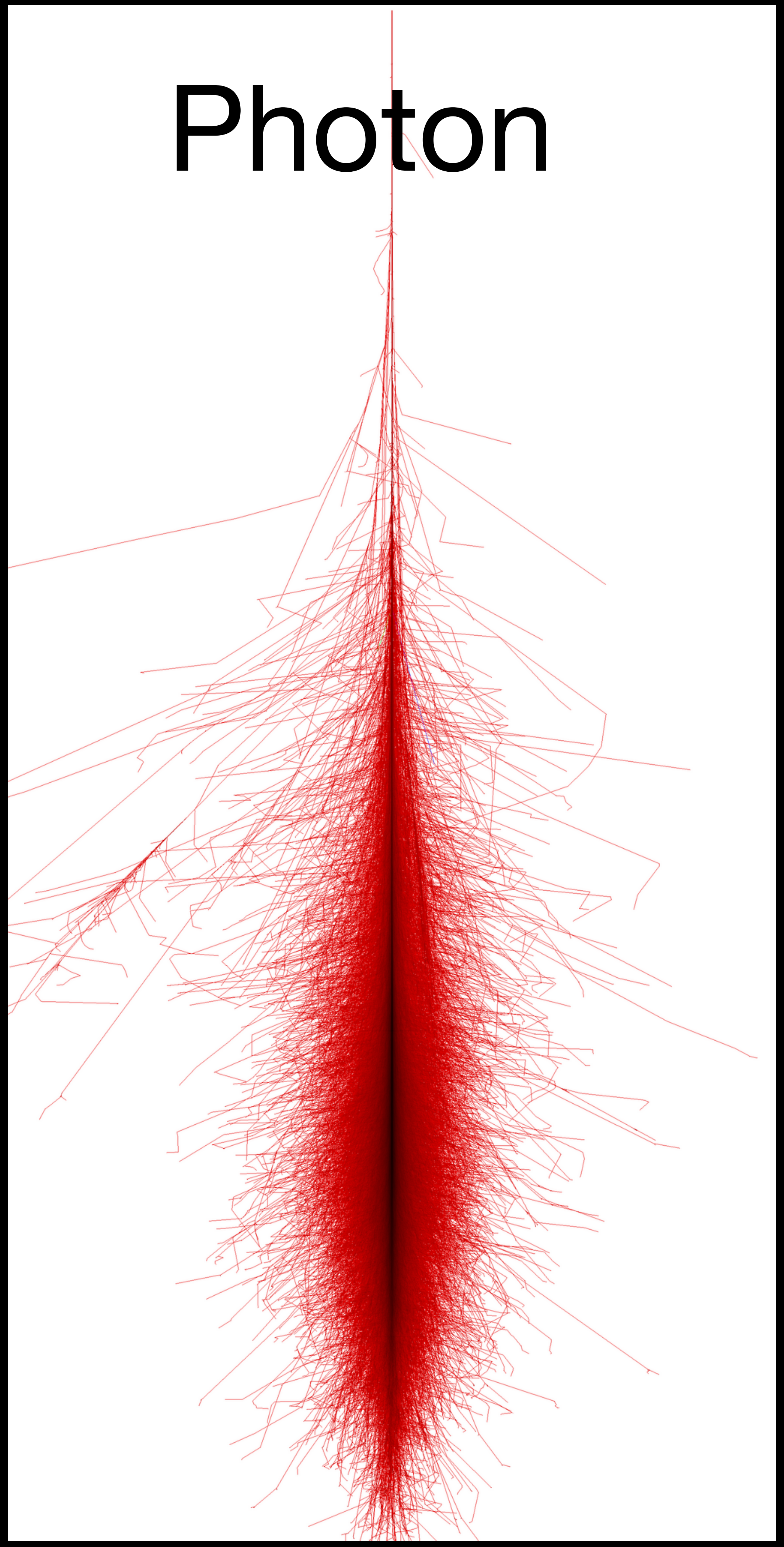

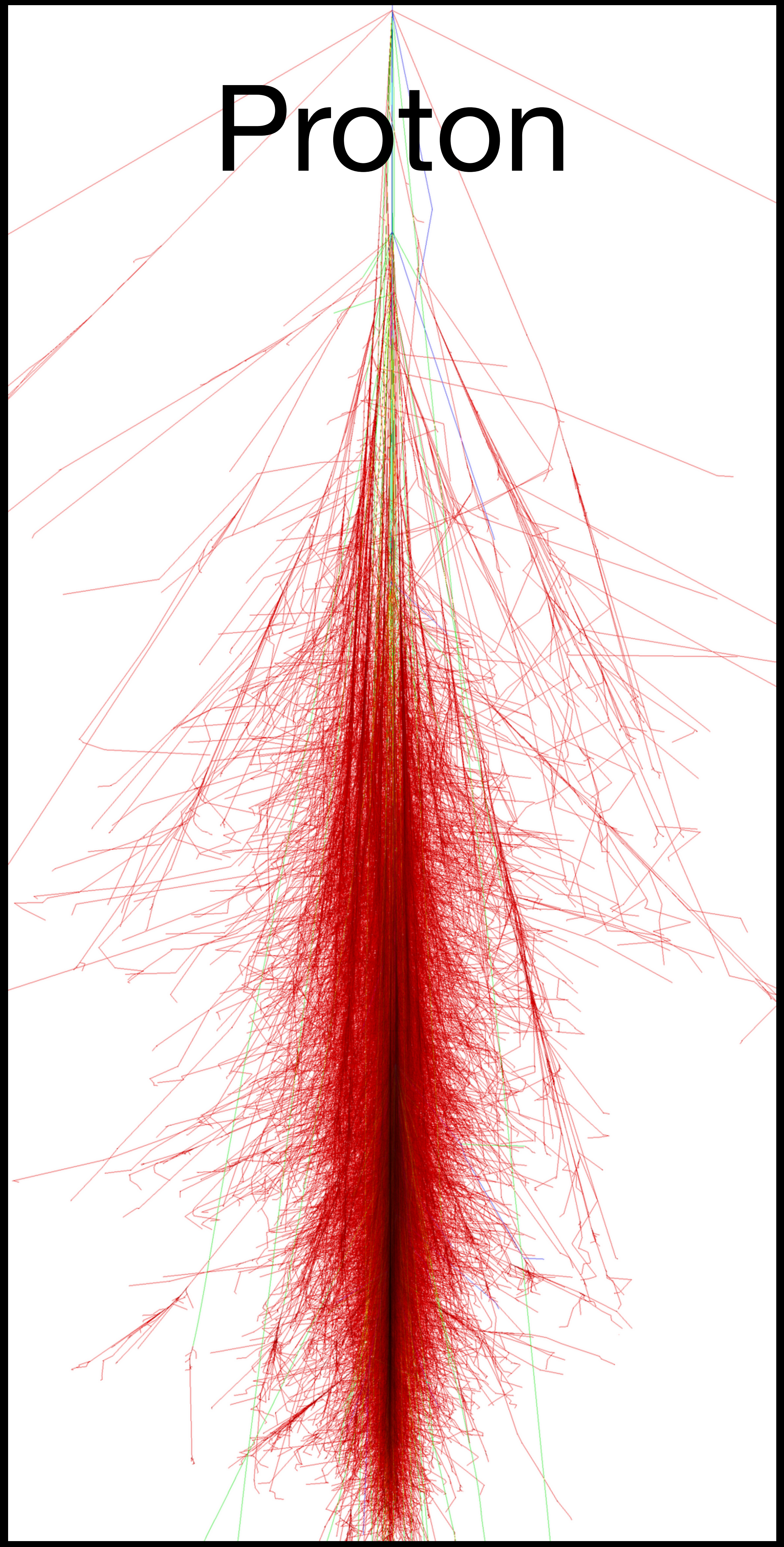

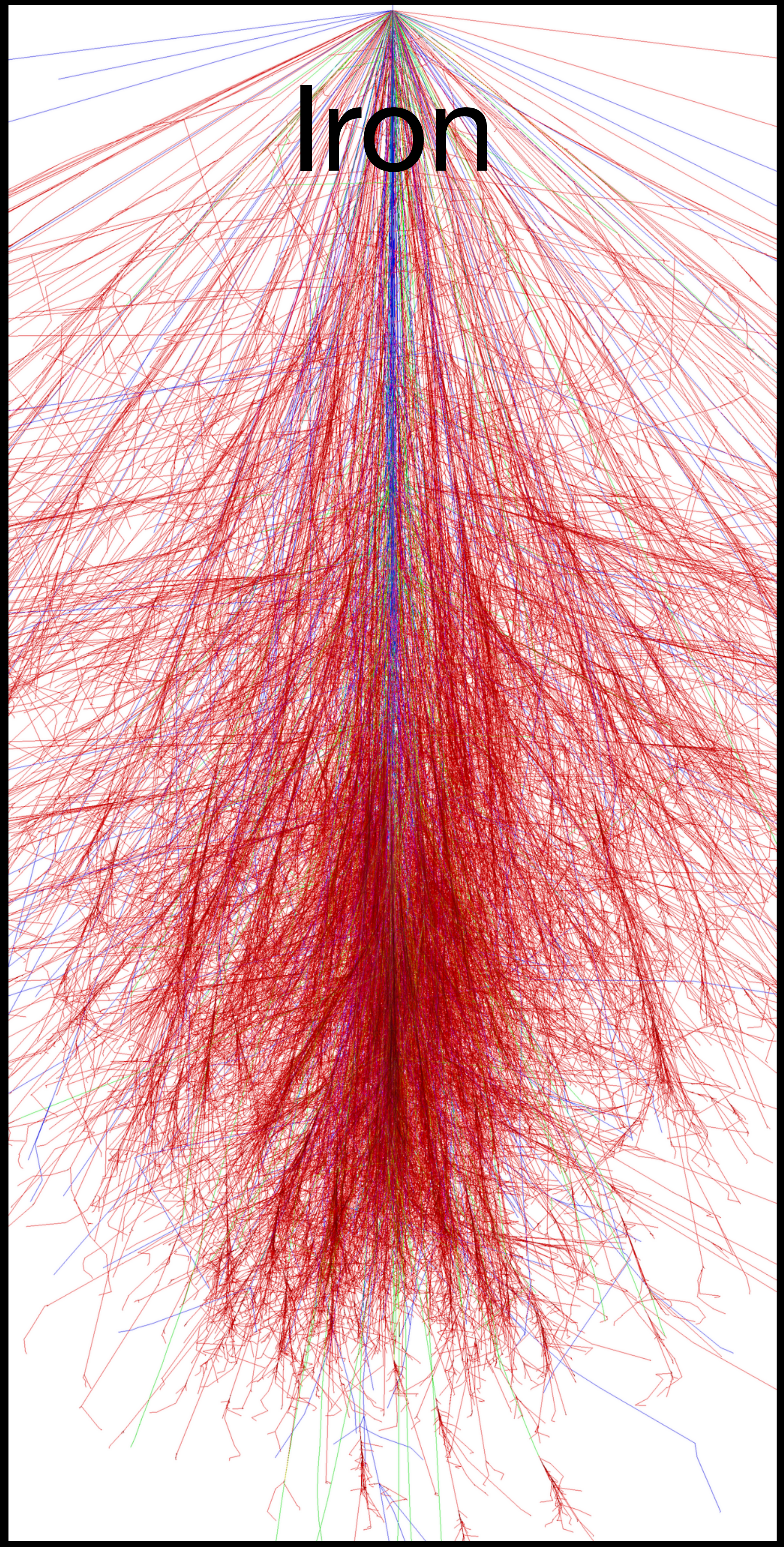

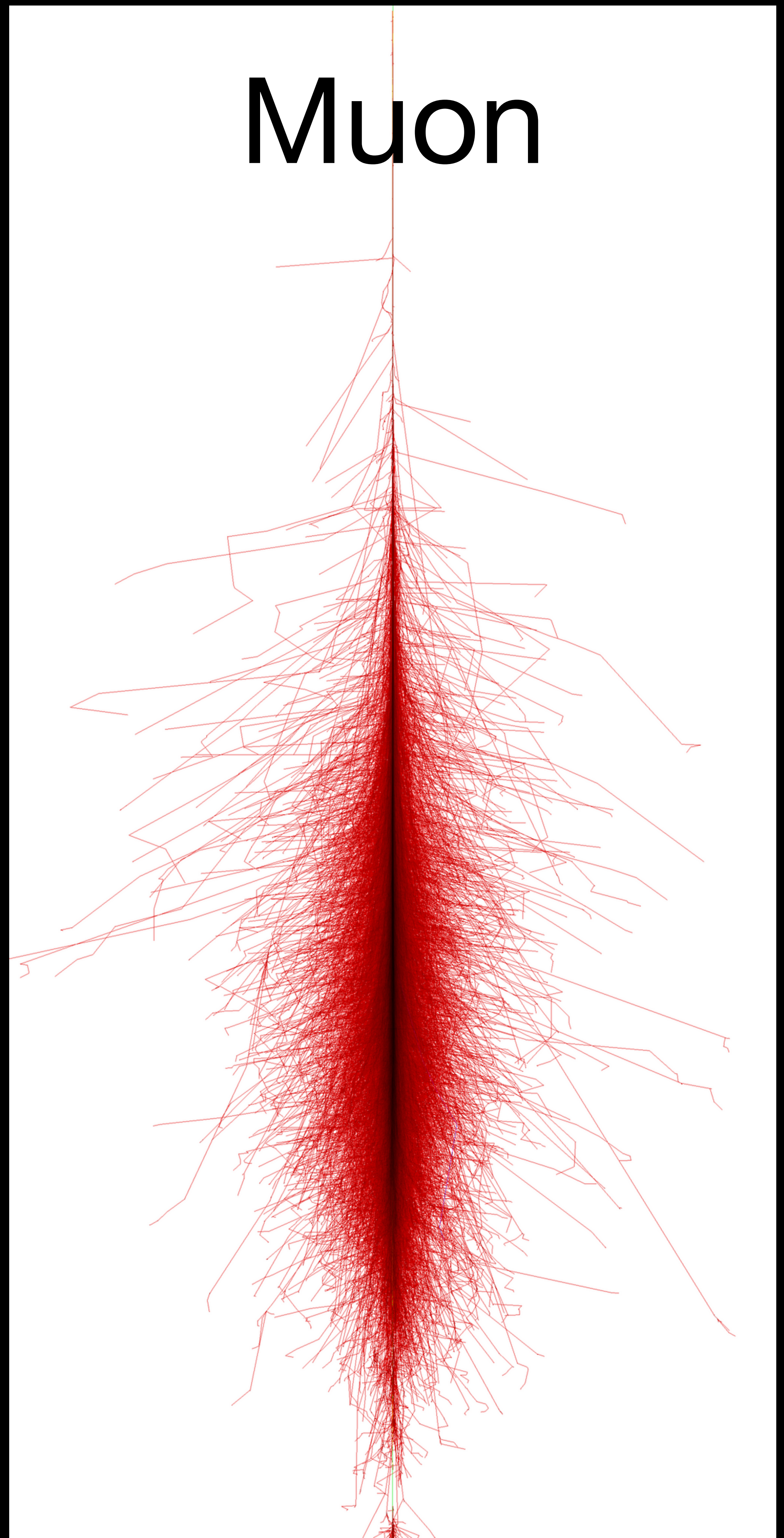

Hadron Showers

- High energy hadrons form particle showers when passing through dense material

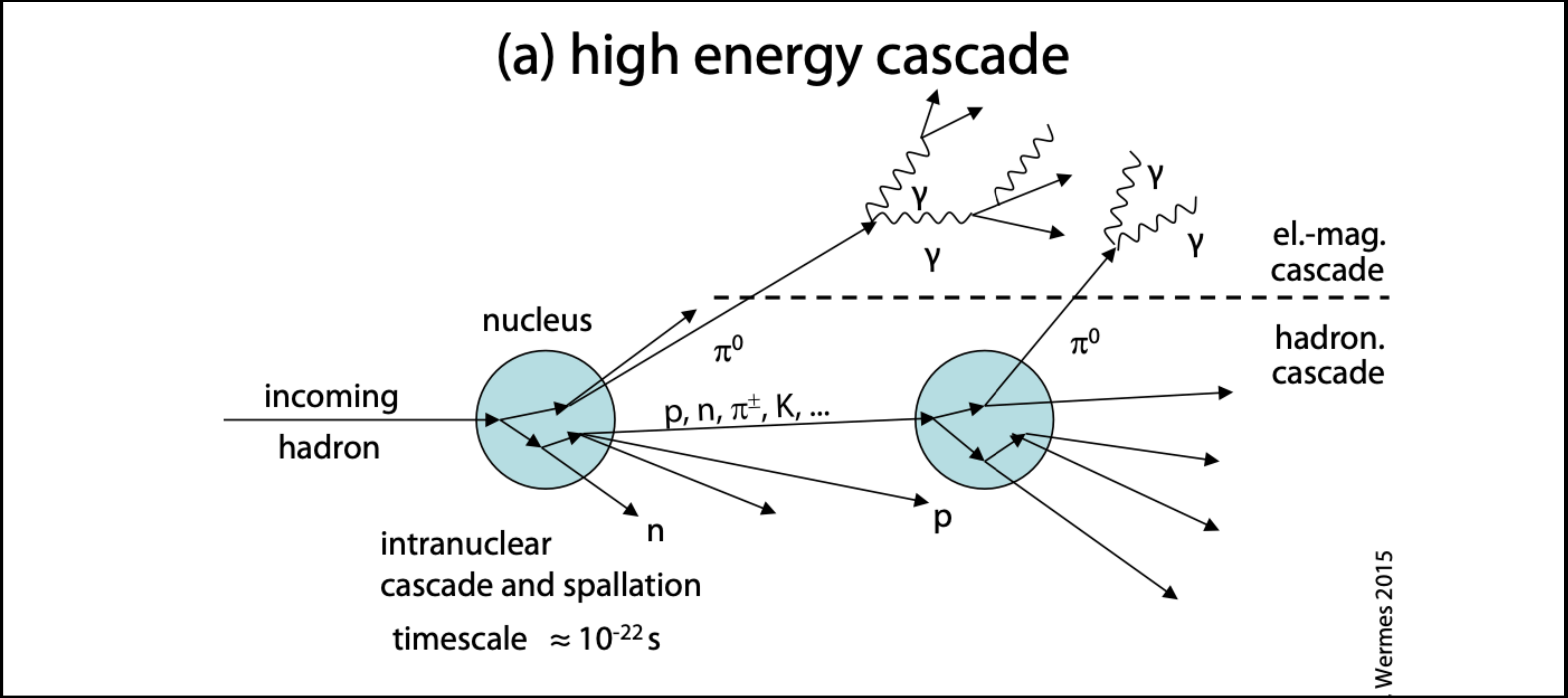

Spallation: The excited nucleus releases its energy through emission of nucleons

Shower components and shower fluctuations

- Shower fluctuations are much stronger in hadronic than electromagnetic showers
- Caused by the splitting of the shower in different components for which the fractions f_i of the total deposited energy strongly fluctuate
- The energy deposited in a block of matter consists of the following components:
  - $E_{dep} = \left(f_{em} + \underbrace{f_{ion} + f_n + f_\gamma + f_B}_{f_h}\right) E$

Shower components and shower fluctuations

- The hadronic fraction is divided into contributions which differ in the way they are detected:
  - f_{ion}: Charged particles transfer energy to the medium through ionization
  - f_n: Neutrons transfer the energy through elastic collision or nuclear reactions
  - f_γ: The photons from nuclear reactions are allocated to the ‘hadronic’ part of the energy because they arise from nuclear reactions and are strongly correlated with other hadronic energies
  - f_B: The energy which is needed to break up a nucleus, corresponding to its binding energy

Fractions of hadronically deposited energy

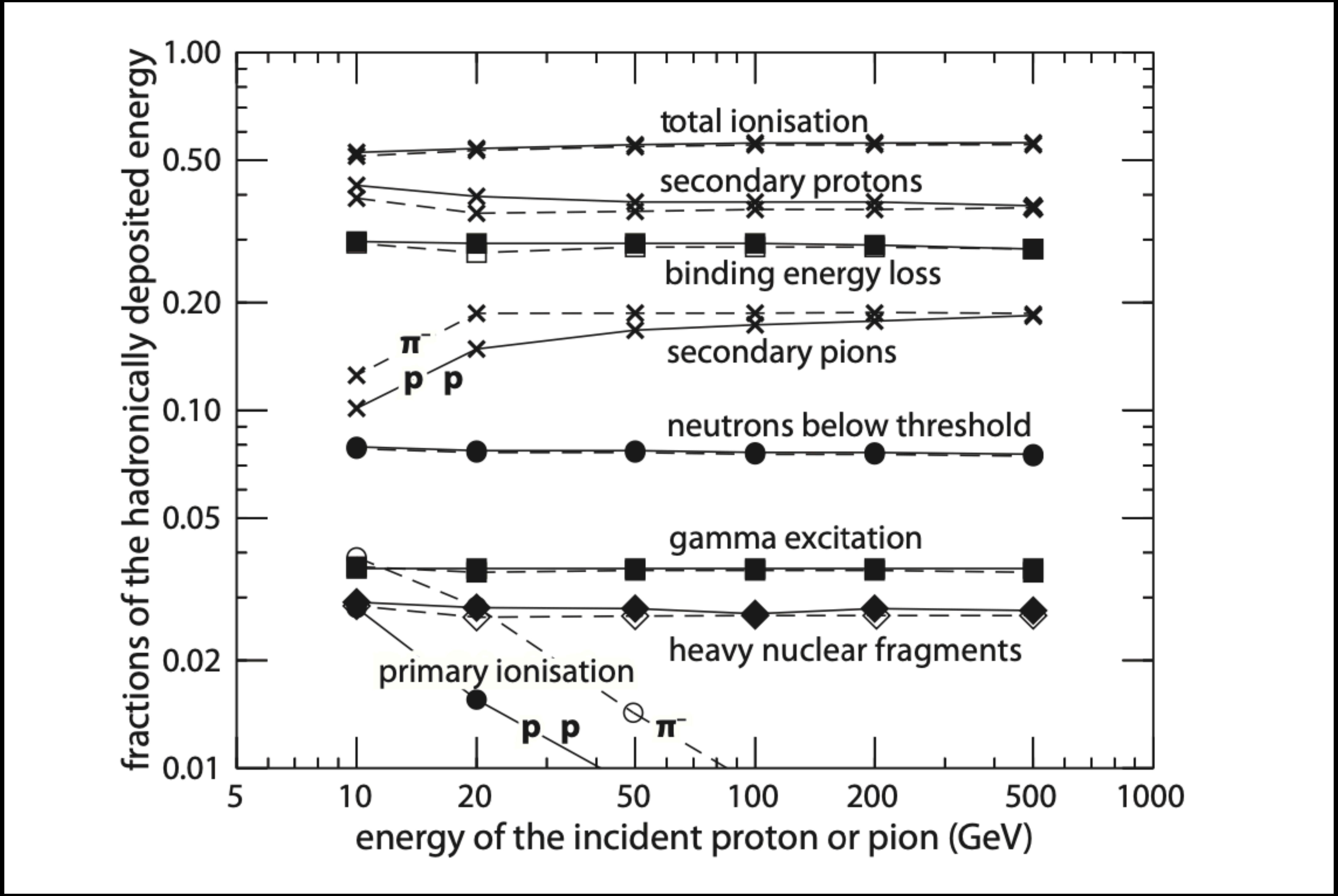

Hadronic Showers Fluctuations

- interesting measurements of the longitudinal energy deposition in em and hadronic showers were made with the “Hanging file calorimeter”

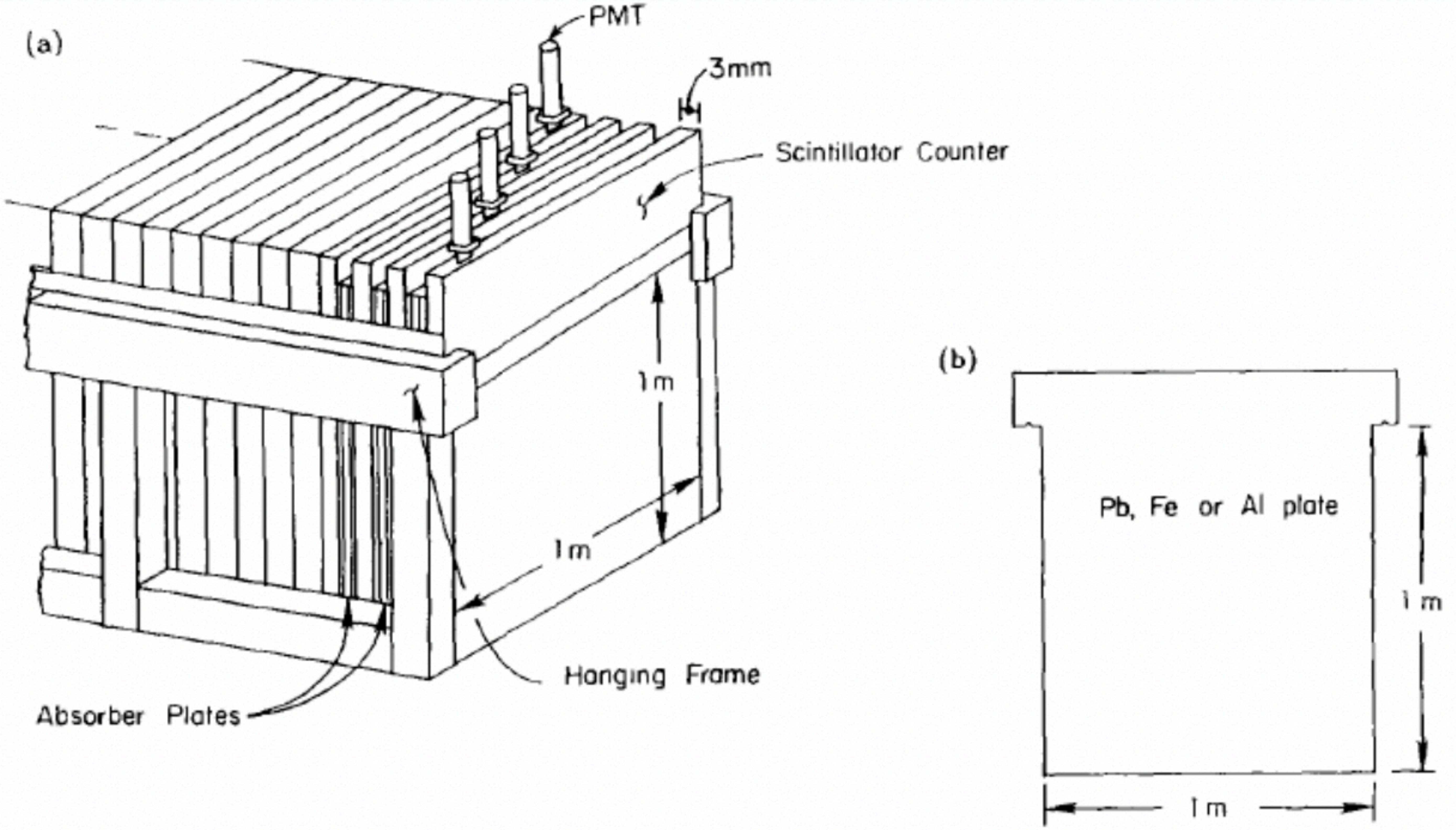

Fig. 1. (a) Schematic overview of the hanging file calorimeter (HFC). There was no transverse segmentation. The maximum depth of the calorimeter can be configured up to 2.2 m with a maximum number of 105 read-out planes. Each scintillator counter was read out separately. (b) Schematic drawing of the absorber plate.

Shower fluctuations

EM Shower Fluctuations

- 170 GeV electrons hit the Hanging file calorimeter
- Longitudinal shower profile is reconstructed by reading out each layer for each event
- EM shower depositions do not fluctuate significantly

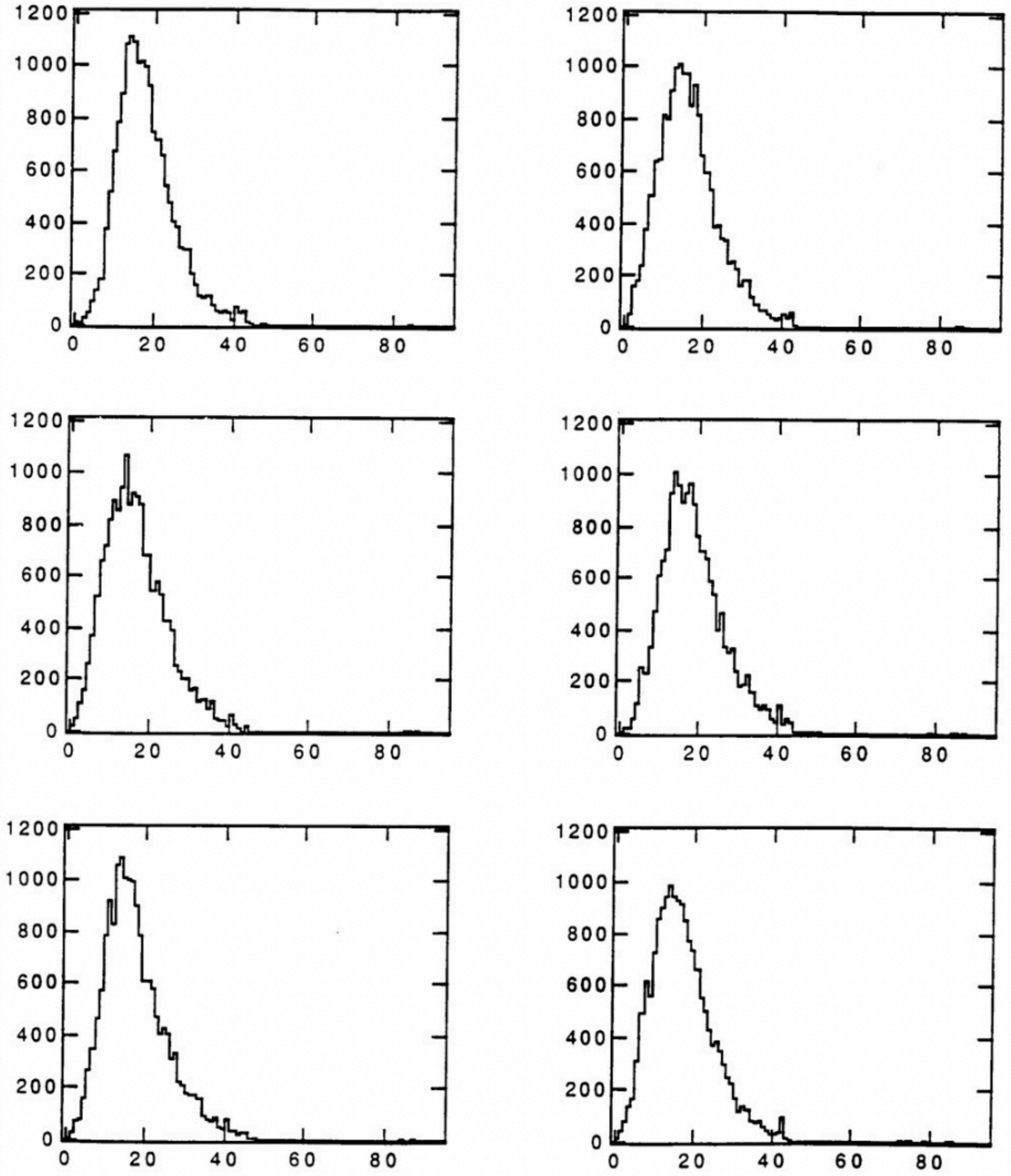

General Principles of Calorimetry

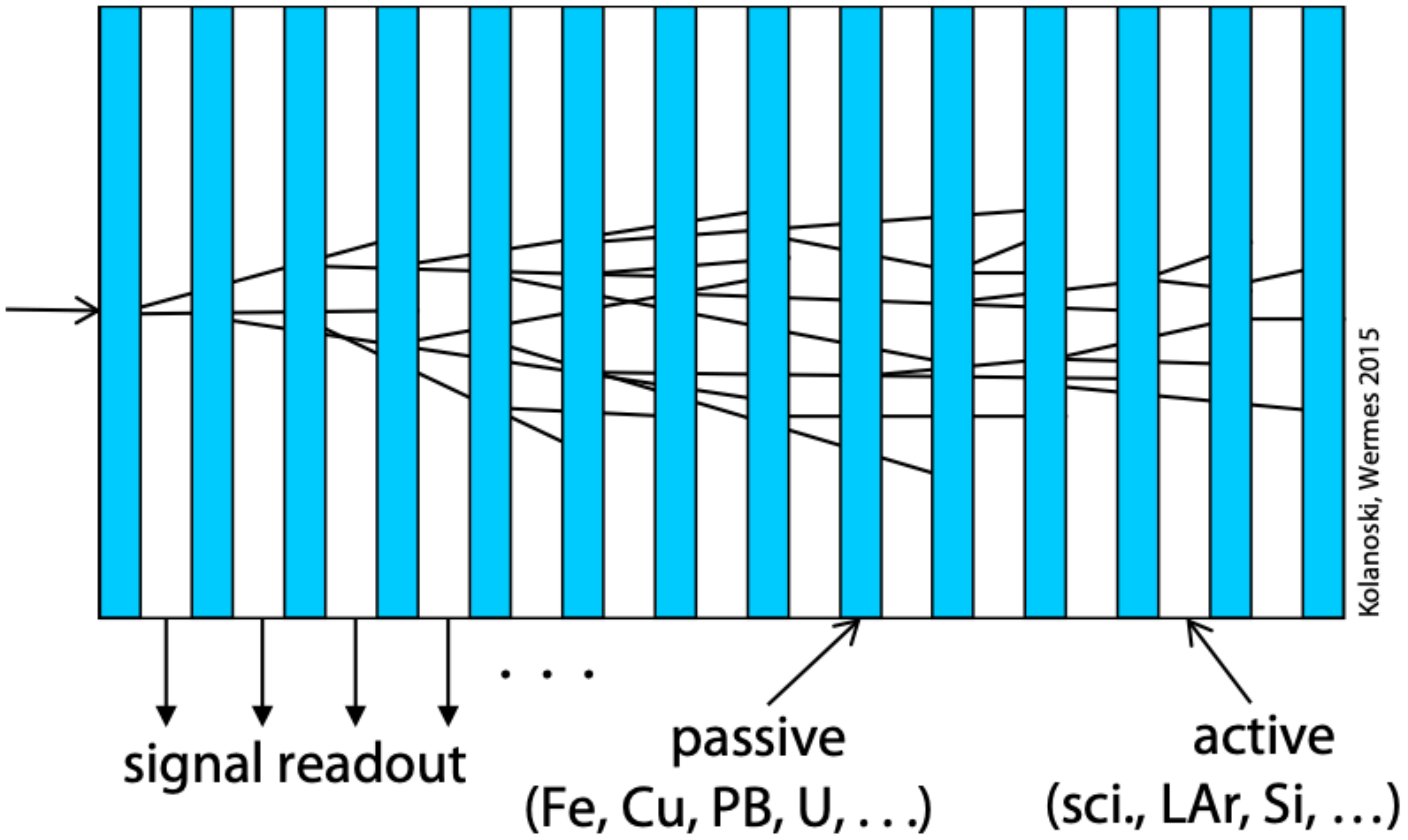

Fig. 15.15 Schematic of a sampling calorimeter, here in a sandwich arrangement.

General Principles of Calorimetry

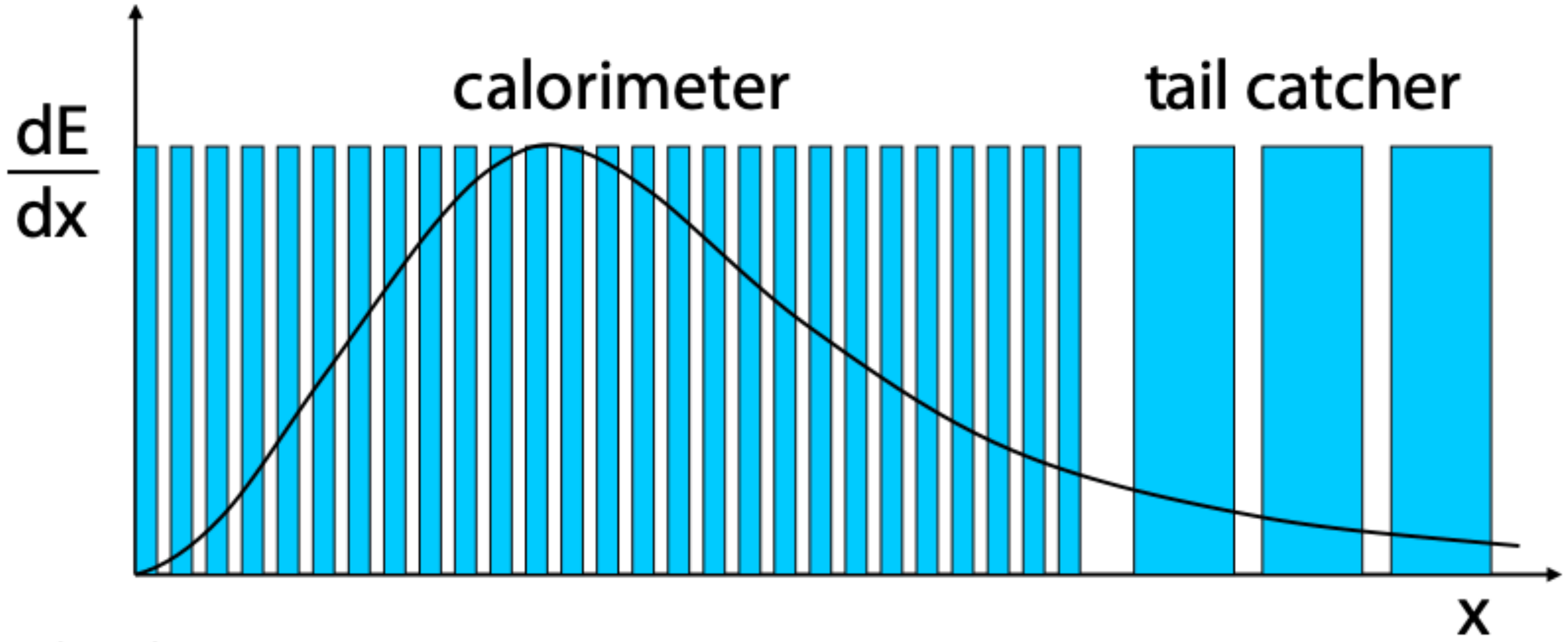

Kolanoski, Wermes 2015

Fig. 15.19 Measurement of the shower loss by means of a subsequent coarser detector (*tail catcher*).

Longitudinal Structure

- Longitudinal segmentation: In electromagnetic calorimeters, a longitudinal segmentation of the signal readout can substantially improve the hadron-electron separation
- Tail catcher: If shower losses cannot be avoided even a quite rough measurement of the loss by a so-called *tail catcher* can cause a distinct improvement of the energy
- Presampler: In front of the calorimeters detectors for tracking and possibly particle identification are often installed. Made of as little material as possible. Actual radiation length in front of the calorimeter can degrade energy resolution. Determines if the shower has started

Energy Resolution

- In most calorimeters the energy resolution is determined by the stochastic fluctuations of the number of charged particles contributing to the signal
- If their number N_S is proportional to the primary energy ($N_S \propto E$), with a standard deviation ($\sqrt{N_S}$) according to Poisson statistics, then the resolution is:
  - $$\frac{\sigma_E}{E} \propto \frac{\sqrt{N_S}}{N_S} = \frac{1}{\sqrt{N_S}} \propto \frac{1}{\sqrt{E}}$$
  - Energy resolution calculated as:
    - $$\frac{\sigma_E}{E} = \sqrt{\frac{a^2}{E} + \frac{b^2}{E^2} + c^2}$$

Energy Resolution

- $$\frac{\sigma_E}{E} = \sqrt{\frac{a^2}{E} + \frac{b^2}{E^2} + c^2}$$
  - a: stochastic fluctuations of the shower development being particularly strong for sampling calorimeters due to incomplete sampling
  - b: electronic noise which contributes $\frac{1}{E}$ term to the relative resolution because the absolute fluctuations are energy independent
  - c: mechanical and electronic imperfections, fluctuations in the leakage losses, inter-calibration errors and others with absolute contributions which rise with energy

Energy Resolution

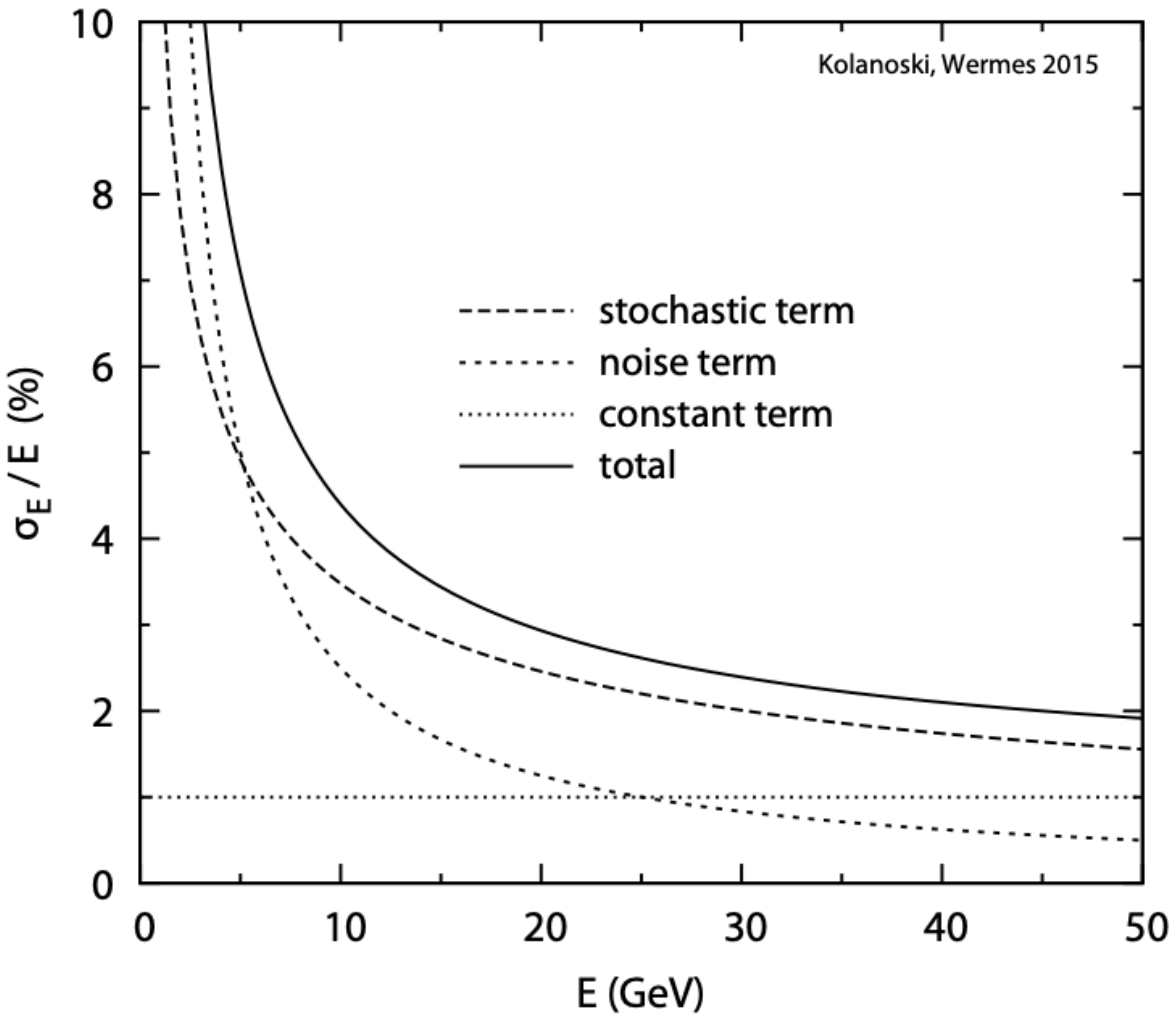

Fig. 15.20 Example for the energy dependence of the energy resolution of a calorimeter with the individual contributions of the resolution terms as given in (15.33), with $a = 0.11/\sqrt{\text{GeV}}$, $b = 250\,\text{MeV}$, $c = 0.01$.

CLD Detector

- CLD Paper: https://arxiv.org/pdf/1911.12230
- Read the paper and we will discuss it in class next Monday

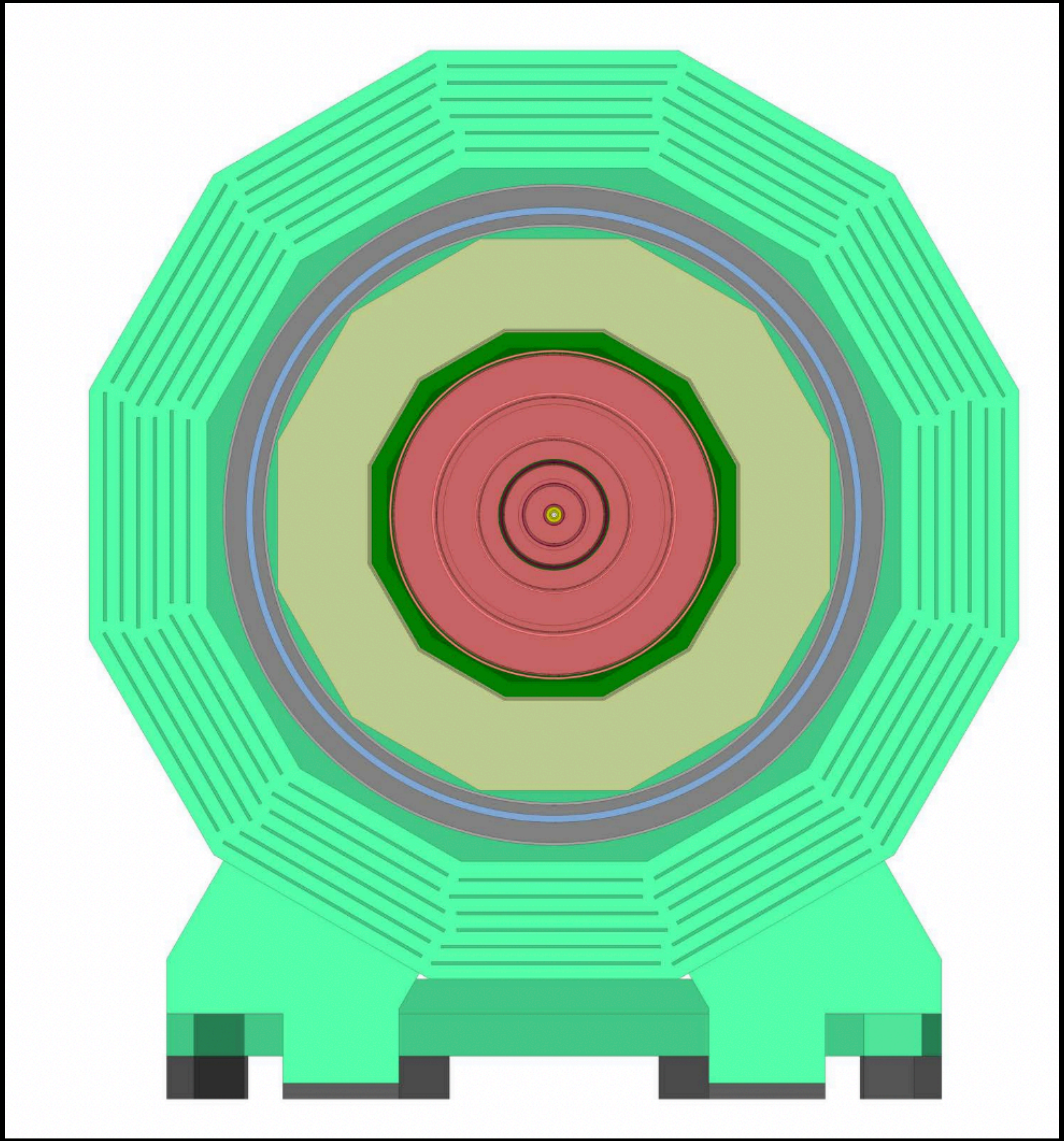

Trigger

Chapter 18

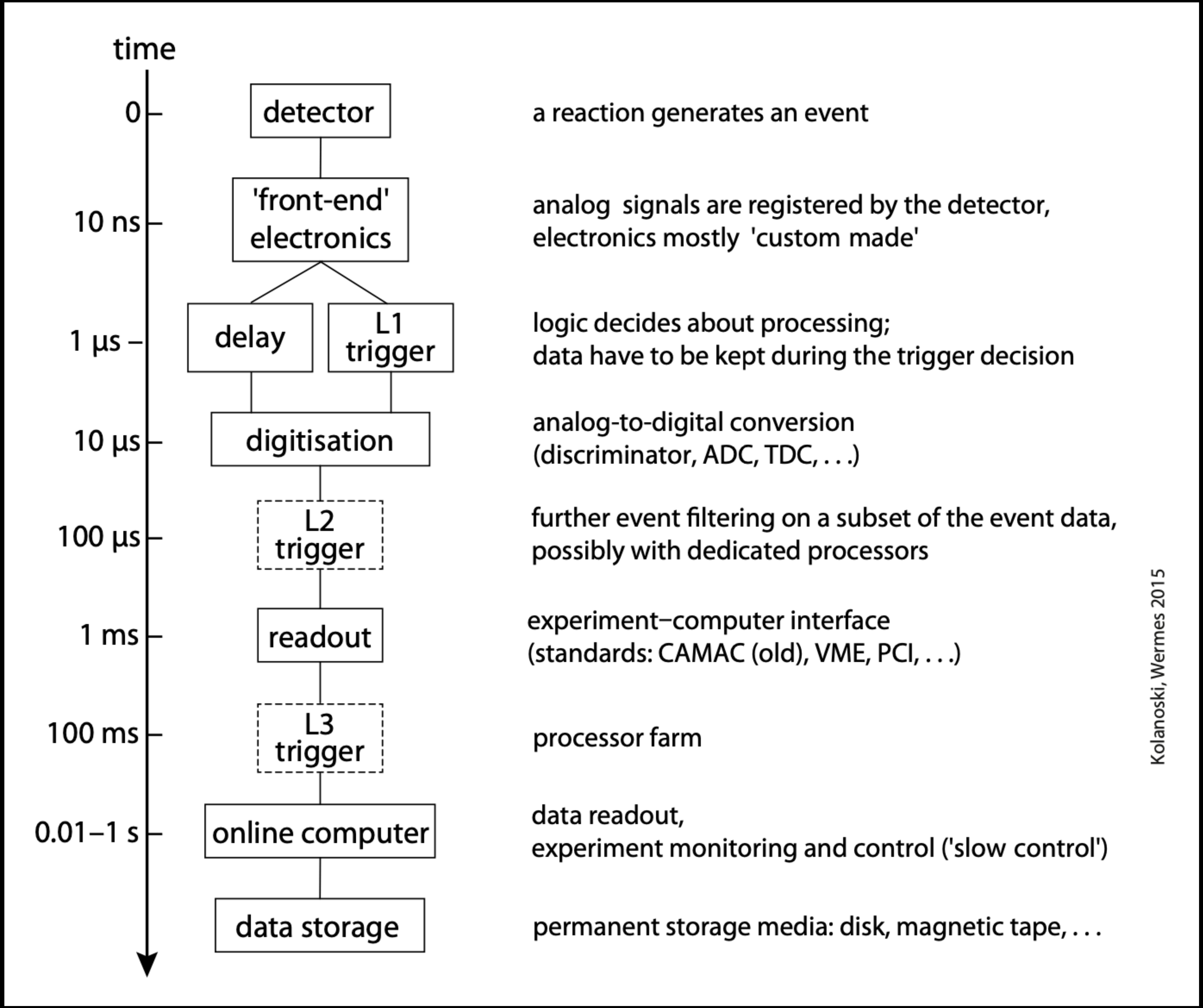

a reaction generates an event

analog signals are registered by the detector,
electronics mostly 'custom made'

logic decides about processing;
data have to be kept during the trigger decision

analog-to-digital conversion
(discriminator, ADC, TDC, . . .)

further event filtering on a subset of the event data,
possibly with dedicated processors

experiment–computer interface
(standards: CAMAC (old), VME, PCI, . . .)

processor farm

data readout,
experiment monitoring and control ('slow control')

permanent storage media: disk, magnetic tape, . . .

Kolanoski, Wermes 2015